

Resonating color state and emergent chromodynamics in the kagome antiferromagnet

O. Cépas and A. Ralko

Institut Néel, CNRS et Université Joseph Fourier, Boîte Postale 166, F-38042 Grenoble cedex 9, France

(Received 22 June 2011; published 25 July 2011)

We argue that the spin-wave breakdown in the Heisenberg kagome antiferromagnet signals an instability of the ground state and leads, through an emergent local constraint, to a quantum dynamics described by a gauge theory similar to that of chromodynamics. For integer spins, we show that the quantum fluctuations of the gauge modes select the $\sqrt{3} \times \sqrt{3}$ Néel state with an on-site moment renormalized by color resonances. We find nonmagnetic low-energy excitations that may be responsible for a deconfinement “transition” at experimentally accessible temperatures which we estimate.

DOI: [10.1103/PhysRevB.84.020413](https://doi.org/10.1103/PhysRevB.84.020413)

PACS number(s): 75.10.Jm

Spin liquids are intriguing states of matter that do not break any symmetry at zero temperature, and were conjectured by Anderson in the form of a resonating valence bond (RVB) liquid.¹ Contrary to conventional magnets which have long-range order and spin-wave excitations described by an effective nonlinear sigma model,² RVB states have emergent gauge excitations.³ Gauge degrees of freedom appear because of local constraints within a low-energy manifold, such as the hard-core constraint for singlets³ or, more generally, some “ice rules.”⁴ As a result, the magnetism can be described in terms of “electrodynamics” and Coulomb phases which find striking experimental realizations in spin-ice systems at finite temperatures.⁴ Recently, experiments on the two-dimensional spin-1/2 Heisenberg kagome compound $\text{ZnCu}_3(\text{OH})_6\text{Cl}_3$ suggest a possible quantum spin-liquid state at zero temperature.⁵ Theoretically for $S = 1/2$ systems, there is indeed evidence for a spin-liquid state,⁶ not inconsistent^{7,8} with a gapless RVB state.⁹ From a different route, the large- S approach provides important insights, such as integer vs half-integer spin effects.¹⁰ For the kagome system, the large- S spin-wave theory is known to break down because of *local* (weathervane) modes with diverging fluctuations.^{11–13} This is the consequence of a macroscopic number of classically degenerate states that can be seen as the three colorings of the kagome lattice with spins pointing at 120° apart (Fig. 1). Contrary to spin-ice models where the constraint is enforced by strong local anisotropies,⁴ here the local (color) constraint arises dynamically because of an order-by-disorder mechanism.^{11–13} In this Rapid Communication, we show that the spin-wave breakdown is the signature of emergent gauge degrees of freedom that are governed by a Hamiltonian similar to that of quantum chromodynamics. The issue is whether the present theory stabilizes a resonating color “crystal” (with a finite Néel order parameter and color resonances) or leads to a delocalization in the low-energy manifold, thus realizing a resonating color “spin liquid” (instead of RVB).

First, we derive the effective lattice gauge theory in the low-energy manifold of three colorings starting from large S . It is known both from classical Monte Carlo simulations ($S = \infty$)^{12,14} and from exact spectra at finite S (Ref. 15) that the three-coloring states (spin-ice subspace) are relevant at low energy. To remain in the low-energy manifold, single spin flips are not allowed and the spin motion consists of the tunneling of a collective loop of spins across an energy barrier separating

degenerate states.¹⁶ The loops are closed loops of L spins of two colors (Fig. 1). Classically, they can be rotated freely about the effective field of the third-color spins, for any arbitrary collective angle ϕ . However, this local rotation can be viewed as a defect for the spin waves, and therefore increases the zero-point energy. In the Born-Oppenheimer approximation, this generates an effective energy barrier for the slow loop motion.^{13,17} We now calculate the energy barrier starting with the quantum Heisenberg Hamiltonian

$$H = J \sum_{(i,j)} S_i S_j, \quad (1)$$

with J the coupling between nearest-neighbor spins S . To do so, we start with a classical ground state and consider a given loop (see Fig. 1, for example) rotated by ϕ . The Holstein-Primakov spin-wave equations of motion are set up in real space (given that translation invariance is broken) and diagonalized for different ϕ (up to $N = 972$ sites). We compute the zero-point energy

$$V_L(\phi) = \sum_{l=1}^N \frac{1}{2} \omega_l(\phi), \quad (2)$$

where l runs over all spin-wave energies, ω_l . It is a double-well potential with two minima located at $\pm\pi/2$ (Fig. 2) corresponding to the selection of three colorings. The potential

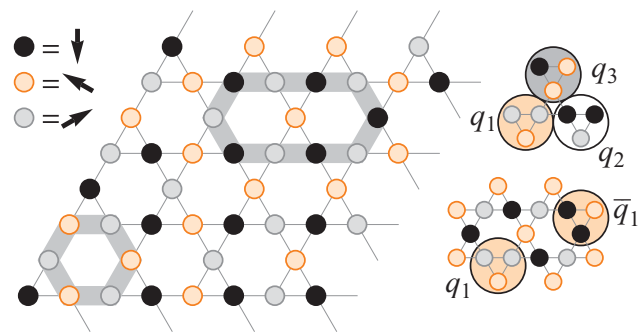


FIG. 1. (Color online) Loop-induced low-energy dynamics within the three-coloring manifold of the kagome lattice (spin/color equivalence is shown), described as “gluon” dynamics. Right: the $q_1 \bar{q}_1$ (“meson”) and $q_1 q_2 q_3$ (“baryon”) are high-energy “matter” excitations violating the local constraint.

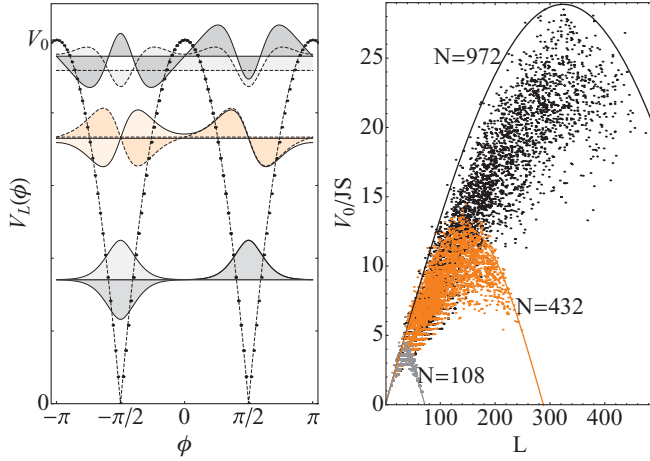


FIG. 2. (Color online) Left: Double-well potential for the loop motion and quantized levels with even (solid line) and odd (dashed line) wave functions. Right: Barrier height distribution as a function of loop length in the three-coloring manifold. The curves shown are simple cosine functions.

is well fitted by an inverted parabolic function, which we will use in the following. Repeating the calculation for loops of arbitrary lengths in a Monte Carlo sampling of the manifold, we have systematically computed the barrier heights V_0 (Fig. 2). For small loops, we find $V_0 = \eta JS L$ with $\eta = 0.14$, in agreement with Ref. 13; the barriers are rather small. For larger loops, a dispersion about the mean value is observed, which tells us that the barrier heights depend on the configuration. Note that the symmetry about $L = N/3$ occurs because rotating a loop of $L = 2N/3$ results in choosing another global plane at no energy cost. We also point out that anharmonic corrections will give additional contributions $\sim JS^{2/3}$.^{16,18,19} The kinetic energy of a loop is obtained by considering the spins of the loop in the effective field of the fixed third-color spins (say along $-z$). The Goldstone mode corresponds to the collective rotation about z and is taken separately.²⁰ Together with V_L we obtain²¹ the Hamiltonian for a single loop,

$$H_L = \frac{1}{2\chi} (\hat{S}^z - A)^2 + V_L(\phi), \quad (3)$$

where $\hat{S}^z = \sum_{i=1}^L S_i^z = -i\partial/\partial\phi$ is the total spin of the loop, conjugate to ϕ , and $\chi = L/(4J)$, the moment of inertia. H_L is similar to an Aharonov-Bohm ring in a double-well potential. The flux $A = LS/2$ is the classical magnetization of the loop. For the kagome lattice, the only possible loops have $L = 4n + 2$ (n an integer),¹⁶ so that $A = (2n + 1)S$. By considering the Berry phase $2\pi A$, von Delft and Henley predicted a destructive interference for half-integer S .¹⁶ Indeed, the first term of Eq. (3) is minimized for $S^z = A$ if A is an integer, or $S^z = A \pm 1/2$ if A is half integer (“Kramers” doublet). In the presence of the external potential, this remains true. By using a simple gauge transformation $\Psi(\phi) = e^{-iA\phi} u(\phi)$, $u(\phi)$ satisfies the Schrödinger equation with either periodic (integer S) or antiperiodic (half-integer S) boundary conditions. $V_L(\phi)$ has a periodicity of π , so we expect Bloch states with energies E_k . Periodic (respectively, antiperiodic) boundary

conditions select the bonding $k = 0$ and antibonding $k = 1$ states (respectively, $k = \pm 1/2$), which have energy difference t_L . Given that $V_L(\phi) = V_L(-\phi)$, we have $E_{-k} = E_k$ and the two states $k = \pm 1/2$ remain degenerate ($t_L = 0$).

To extract t_L , we solve exactly the Schrödinger equation in the double-well parabolic potential with parabolic cylinder wave functions (Fig. 2). In the semiclassical limit (large S or large L), the solution coincides with the Wentzel-Kramers-Brillouin approximation and we obtain

$$\begin{cases} t_L = aJ \exp\left(-\frac{\pi^2}{4}\sqrt{\eta S/2L}\right) & (\text{integer } S) \\ t_L = 0 & (\text{half-integer } S), \end{cases} \quad (4)$$

where $a = 0.261(\eta S)^{11/12} L^{5/6}$ and $\eta = V_0/JSL$, i.e., neglecting the dispersion of the barrier heights. Quantum tunneling of loops of size $L > L_c = 4/\pi^2\sqrt{\eta S}$ is therefore suppressed.

We now consider the resulting low-energy dynamics on the lattice. In this derivation, the lowest energy states are the three-coloring quantum coherent states $|C\rangle$.²² The number of states scales like $W \sim 1.13^N$ in the thermodynamic limit^{23,24} and is much smaller than that of the original spin problem (1), $(2S + 1)^N$. The dynamics of the loops is described by the quantum Hamiltonian

$$H_e = - \sum_{C,C'} t_{C,C'} |C\rangle\langle C'| + \sum_C E_C |C\rangle\langle C|, \quad (5)$$

where $t_{C,C'} = t_L$ if the two states $|C\rangle$ and $|C'\rangle$ are connected by the tunneling of a loop of size L and $t_{C,C'} = 0$ otherwise. The model depends only on S and the largest energy scale is $t_6 \equiv t$. Anharmonicity^{18,19} and further neighbor couplings generate a finite E_C and phase competitions that are beyond the scope of this Rapid Communication²¹ (here $E_C = 0$). To rewrite H_e exactly in terms of exchange operators of three colors, we have to use the 3×3 Gell-Mann matrices $\lambda_{c=1,2,3}^\pm$ of the $SU(3)$ algebra. We find

$$H_e = -t_6 \sum_{\square} \sum_{c=1}^3 \lambda_{c,1}^+ \lambda_{c,2}^- \lambda_{c,3}^+ \lambda_{c,4}^- \lambda_{c,5}^+ \lambda_{c,6}^- + \text{H.c.} + \dots, \quad (6)$$

where the dots stand for longer loops. The Hamiltonian (6) is a pure lattice gauge model describing the loop dynamics, and is similar to that of quantum chromodynamics with the local $SU(3)$ symmetry broken to $U(1) \times U(1)$.²⁵ The weathervane modes can therefore be seen as “gluons.” Note that the use of the eight operators of $SU(3)$ is necessary because here, contrary to Ref. 26, the Hamiltonian respects the global Z_3 symmetry and flips the three types of loops. If we pursue the analogy, the finite-energy excitations are defects in the ice rule that consist of (i) flipping two colors along a finite string;²⁷ it can be seen as a “quark-antiquark” $q_i \bar{q}_i$ (meson) (Fig. 1). In terms of spin, it is a nonmagnetic pair of domain walls with irrational magnetization $\sqrt{3}(\hat{e}_i, -\hat{e}_i)$ (\hat{e}_i are three unit vectors with $\hat{e}_1 + \hat{e}_2 + \hat{e}_3 = 0$). (ii) Permuting a triangle, this generates three quarks in a color singlet $q_1 q_2 q_3$ or $\bar{q}_1 \bar{q}_2 \bar{q}_3$ (baryon), or, in the spin language, a nonmagnetic excitation $\sqrt{3}(\hat{e}_1, \hat{e}_2, \hat{e}_3)$. These are exactly the first excitations of the Potts model, whereas there are other excitations for the Heisenberg model. Below we will address the issue of confinement of these excitations. Finally, we point out that H_e has a complex topological structure separated in Kempe²⁸ and topological sectors.²⁹ While topological sectors can be connected only

by flipping *winding* loops, Kempe sectors are ensembles of topological sectors that cannot be connected by such global moves.^{28,30}

The ground state is in general a resonating color state, $\Psi = \sum_C A_C |C\rangle$ in a given sector and the issue is whether it breaks the Z_3 symmetry or not. There is an extension of the model for which Ψ is known exactly. By adding $E_C = U_L n_L(C)$, which penalizes states with a large number $n_L(C)$ of loops of size L , one obtains a Rokhsar-Kivelson (RK) model for color dimers.²⁹ In this case, the ground state is the resonating color ‘spin liquid’, $\Psi = \sum_C |C\rangle$, in each topological sector at the RK point, $U_L = t_L$.²⁹ We study model (6) with $E_C = 0$ by Lanczos exact diagonalization of clusters of size $N = 27, 36, 54, 81, 108$ and $T = 0$ quantum Monte Carlo (up to $N = 675$), since H_e is free of the sign problem. We find that (i) Ψ belongs to the largest topological and Kempe sector (which is nondegenerate and has all topological numbers equal to $l/3$, where l is the linear dimension). (ii) Ψ has larger amplitudes onto the six $\sqrt{3} \times \sqrt{3}$ states, and a finite associated Néel order parameter m^2 , which extrapolates to a finite value for infinite size, $m_\infty \sim 0.63\text{--}0.68$, depending weakly on L_c (Fig. 3). To confirm the Néel order, we also calculate the low-energy spectrum by exact diagonalization. For such a discrete broken symmetry, we expect six quasidegenerate states separated from higher energy states. While there is no clear separation of scale, the gap does decrease as $\exp(-\alpha N^{1/2})$ which reflects the development of a macroscopic energy barrier (Fig. 4). The low-energy spectrum is therefore perfectly compatible with a Néel order with the same pattern as predicted earlier,^{18,19,31} and on-site magnetization renormalized by color fluctuations. However, there are unconventional nonmagnetic excitations at low energy of order t (gluons) which bear some similarity with the low-lying states of exact spectra.^{15,32}

To discuss the consequences of these unconventional excitations and analyze these results more quantitatively, we consider the effective gauge theory in the continuum limit.

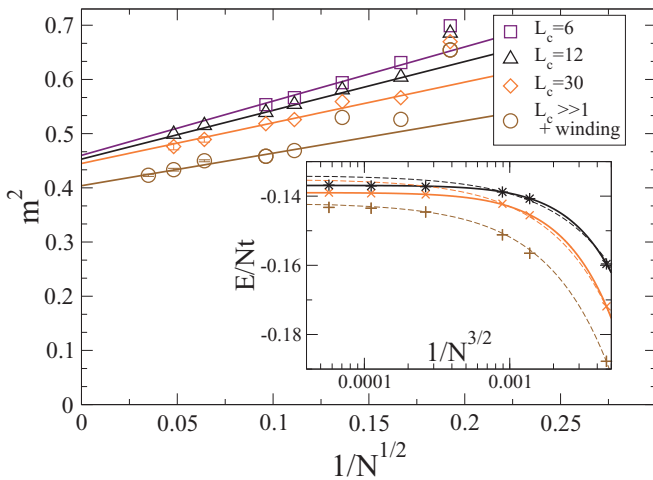


FIG. 3. (Color online) Finite-size scaling of the order parameter of the $\sqrt{3} \times \sqrt{3}$ Néel state, extrapolating to a finite value (exact diagonalization and quantum Monte Carlo). Inset: total energy and fits assuming gapped (solid lines) or gapless (dashed lines) excitations.

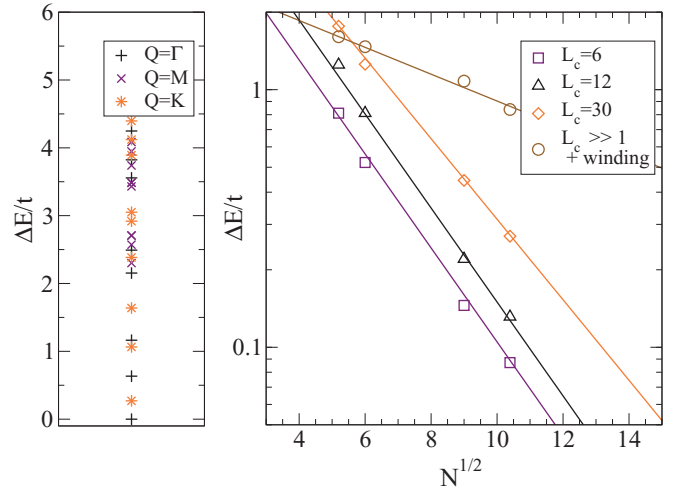


FIG. 4. (Color online) Left: energy spectrum ($N = 108$) showing no clear separation of scale. Right: the lowest *finite-size* gap follows $\Delta E/t \sim \exp(-\alpha N^{1/2})$, confirming the broken symmetry of the $\sqrt{3} \times \sqrt{3}$ Néel order.

The ice rule provides an exact mapping of the discrete states onto two-component height vectors $\mathbf{h}(r)$ living on the dual lattice.^{27,30,33} For instance, the six $\sqrt{3} \times \sqrt{3}$ states map onto flat interfaces. At $T = 0$, the simplest action compatible with the symmetries is a sine-Gordon model,

$$S = \frac{K}{2c^2} \int d^2 \mathbf{x} d\tau \left[(\partial_\tau \mathbf{h})^2 + c^2 (\nabla \mathbf{h})^2 + \frac{\Delta^2}{2\pi^2} \sum_{\alpha=1}^3 \cos(\mathbf{Q}_\alpha \cdot \mathbf{h}) \right], \quad (7)$$

where K is the stiffness, Δ^2 is the amplitude of the locking potential, and $|\mathbf{Q}_\alpha| = 4\pi/\sqrt{3}$.^{27,30,33} Classical minima of Eq. (7) correspond to the ‘‘flat’’ $\sqrt{3} \times \sqrt{3}$ Néel states, with zero-point oscillations described by the two ‘‘gluon’’ modes $\omega_{\mathbf{q}} = (c^2 \mathbf{q}^2 + \Delta^2)^{1/2}$. At $T = 0$ and in $(2+1)$ dimensions, no quantum phase transition is expected.³⁴ The gluons mediate an interaction between the defects (quarks) that is confining if Δ is finite as $V(r) \sim \Delta r$.³⁵ To obtain these parameters, we have used the finite-size correction to the total energy, $\frac{E}{N} = e_0 - 0.6586 \frac{2c}{N^{3/2}}$, for a hexagonal lattice of N sites, without a gap (dashed line in Fig. 4). We clearly see that the fit is improved at large distances (for a finite L_c) by using $\frac{1}{N^{3/2}} \exp(-l/\xi)$, where $\xi = c/\Delta$ gives the confinement scale (solid line), and $c = 13.4t$, $\xi = 15.5$, and $e_0 = -0.1430t$. To estimate the stiffness we calculate the order parameter, $m_\infty = \langle e^{i\mathbf{Q} \cdot \mathbf{h}} \rangle$, with $|\mathbf{Q}| = 4\pi/3$.^{27,30,33} Assuming a small gap, $m_\infty = e^{-(1/2)\mathbf{Q}^2 \langle \mathbf{h}^2 \rangle} = e^{-(8\pi c/9K)}$, and by using $m_\infty \sim 0.65$, we extract $K \sim 90t$.

Thermal effects. We first discuss the thermal restoration of the discrete symmetry of the effective model: the interface described by Eq. (7) undergoes a roughening transition in the Kosterlitz-Thouless universality class (triggered by the condensation of gluons) at a critical temperature, usually obtained from the scaling dimension of the locking potential, $2 - |\mathbf{Q}_\alpha|^2 T/4\pi K$, leading to $T_c = 3K/(2\pi)$. For $T < T_c$ the

system breaks the discrete Z_3 symmetry with a $\sqrt{3} \times \sqrt{3}$ state, the weathervane modes (gluons) are gapped, and the defects (quarks) are confined. For $T > T_c$ the Z_3 symmetry is restored; it is a critical quark-gluon plasma with gapless gluons ($\eta = 4/3$,³⁰ hence a dynamical response $\chi''(\omega) \sim \omega^{\eta/2-1}$). For integer spins, we estimate $T_c/J = 0.16J$ ($S = 1$), $0.06J$ ($S = 2$), 0.02 ($S = 3$), etc., by using $K \sim 90t$ and Eq. (4). For half-integer spins, since $t = 0$ (at the one-loop order) and $t \ll t_6$ (with two-loop cotunneling),²¹ the system is immediately in its infinite temperature phase and is critical. Could this deconfinement transition manifest itself experimentally? The transition should indeed occur in the corresponding spin-ice system with a discrete symmetry. In model (1) with SU(2) symmetry, the Mermin-Wagner theorem ensures that no continuous symmetry breaking will occur at finite temperature: the propagating spin waves induce a finite correlation length, $\xi_{2d} \sim \exp(\rho/T)$,² which cuts off the

infrared divergence of the Kosterlitz-Thouless transition.³⁶ Strictly speaking, T_c is a crossover temperature between two paramagnets. However, the usual thermodynamic singularities will remain sharp because $\xi_{2d} \sim \exp(JS^2/T_c)$ is very large at $T = T_c$.

In conclusion, we argued that the Heisenberg kagome antiferromagnet has long-range Néel order at $T = 0$ for integer spins. Its magnetism is unconventional due to an underlying emergent chromodynamics: there are color fluctuations and additional low-energy excitations described as gapped “gluons” which may condense at T_c (“quark” deconfinement). For half-integer spins, $T_c = 0$ at the lowest order. The difference between half-integer and integer spins reflects the essential quantum nature of the local modes.

We would like to thank P. Bruno, B. Canals, J. Jacobsen, K. Nguyen, and T. Ziman for discussions.

¹P. W. Anderson, *Mater. Res. Bull.* **8**, 153 (1973).

²S. Chakravarty, B. I. Halperin, and D. R. Nelson, *Phys. Rev. B* **39**, 2344 (1989).

³G. Baskaran and P. W. Anderson, *Phys. Rev. B* **37**, 580 (1988).

⁴For a review, see M. J. P. Gingras, *Highly Frustrated Magnetism*, edited by C. Lacroix, P. Mendels, and F. Mila (Springer-Verlag, Berlin, 2010); R. Moessner and K. S. Raman, *ibid.*

⁵For a review, see P. Mendels and F. Bert, *J. Phys. Soc. Jpn.* **79**, 011001 (2010).

⁶S. Yan, D. A. Huse, and S. R. White, *Science* **332**, 1173 (2011).

⁷P. Sindzingre and C. Lhuillier, *Europhys. Lett.* **88**, 27009 (2009).

⁸H. Nakano and T. Sakai, *J. Phys. Soc. Jpn.* **80**, 053704 (2011).

⁹M. B. Hastings, *Phys. Rev. B* **63**, 014413 (2000); Y. Ran, M. Hermele, P. A. Lee, and X.-G. Wen, *Phys. Rev. Lett.* **98**, 117205 (2007).

¹⁰F. D. M. Haldane, *Phys. Rev. Lett.* **50**, 1153 (1983).

¹¹A. B. Harris, C. Kallin, and A. J. Berlinsky, *Phys. Rev. B* **45**, 2899 (1992).

¹²J. T. Chalker, P. C. W. Holdsworth, and E. F. Shender, *Phys. Rev. Lett.* **68**, 855 (1992).

¹³I. Ritchey, P. Chandra, and P. Coleman, *Phys. Rev. B* **47**, 15342 (1993).

¹⁴J. N. Reimers and A. J. Berlinsky, *Phys. Rev. B* **48**, 9539 (1993).

¹⁵I. Rousochatzakis, A. M. Läuchli, and F. Mila, *Phys. Rev. B* **77**, 094420 (2008).

¹⁶J. von Delft and C. L. Henley, *Phys. Rev. B* **48**, 965 (1993).

¹⁷B. Douçot and P. Simon, *J. Phys. A* **31**, 5855 (1998).

¹⁸A. V. Chubukov, *Phys. Rev. Lett.* **69**, 832 (1992).

¹⁹C. L. Henley, *Phys. Rev. B* **80**, 180401(R) (2009).

²⁰See, for a general magnetic field, A. E. Trumper, L. Capriotti, and S. Sorella, *Phys. Rev. B* **61**, 11529 (2000).

²¹O. Cépas and A. Ralko (to be published).

²²The overlap of two states is at most 4^{-L_S} .

²³R. J. Baxter, *J. Math. Phys.* **11**, 784 (1970).

²⁴For finite N , W is not known exactly, except $W = 120$ for $N = 27$; J. Jacobsen and K. Nguyen (private communication).

²⁵ $[U_c, H_e] = 0$ for all local operators, $U_c = \exp[i\alpha \sum_{\Delta} \lambda_{c,i}^z]$, where $c = 3, 8$ is the index of the Gell-Mann matrices.

²⁶C. Xu and J. E. Moore, *Phys. Rev. B* **72**, 064455 (2005).

²⁷J. Kondev and C. L. Henley, *Nucl. Phys. B* **464**, 540 (1996).

²⁸B. Mohar and J. Salas, *J. Stat. Mech.* P05016 (2010).

²⁹C. Castelnovo, C. Chamon, C. Mudry, and P. Pujol, *Phys. Rev. B* **72**, 104405 (2005).

³⁰D. A. Huse and A. D. Rutenberg, *Phys. Rev. B* **45**, 7536 (1992).

³¹S. Sachdev, *Phys. Rev. B* **45**, 12377 (1992).

³²C. Waldtmann, H.-U. Everts, B. Bernu, C. Lhuillier, P. Sindzingre, P. Lecheminant, and L. Pierre, *Eur. Phys. J. B* **2**, 501 (1998).

³³S. E. Korshunov, *Phys. Rev. B* **65**, 054416 (2002).

³⁴J. M. Kosterlitz, *J. Phys. C* **10**, 3753 (1977); J. Zittartz, *Z. Phys. B* **31**, 63 (1978).

³⁵A. M. Polyakov, *Nucl. Phys. B* **120**, 429 (1977).

³⁶If H has a U(1) symmetry, below T_c , the state is critical, implying a second transition.³³